The focusing performance of an aperiodic double layer metallic grating

Ma, Long; Lin, Jie; Jin, Peng; Prewett, Philip; Lu, Zhengang; Tan, Jiubin

DOI:
10.1016/j.mee.2014.05.033

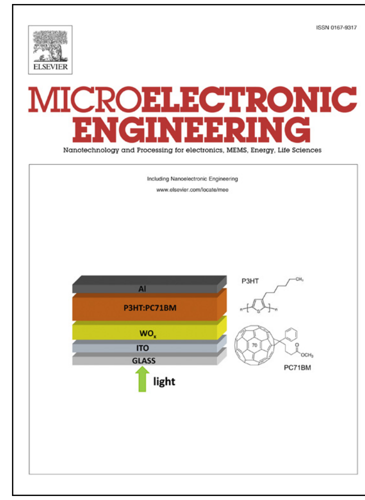

The focusing performance of an aperiodic double layer metallic grating

Long Ma, Jie Lin, Peng Jin, Phil Prewett, Zhengang Lu, Jiubin Tan

PII: S0167-9317(14)00240-8
DOI: http://dx.doi.org/10.1016/j.mee.2014.05.033
Reference: MEE 9482

To appear in: *Microelectronic Engineering*

Received Date: 20 October 2013
Revised Date: 14 May 2014
Accepted Date: 23 May 2014

Please cite this article as: L. Ma, J. Lin, P. Jin, P. Prewett, Z. Lu, J. Tan, The focusing performance of an aperiodic double layer metallic grating, *Microelectronic Engineering* (2014), doi: http://dx.doi.org/10.1016/j.mee.2014.05.033

The focusing performance of an aperiodic double layer metallic grating

Long Ma[a], Jie Lin[a], Peng Jin[a]*, Phil Prewett[b], Zhengang Lu[a], Jiubin Tan[a]

[a] Center of Ultra-precision Optoelectronic Instrument, Harbin Institute of Technology, Harbin 150080, China

[b] School of Mechanical Engineering, University of Birmingham, Edgbaston, Birmingham B15 2TT, UK

*Corresponding author. Building D, NO.2 Yikuang Street, Nangang district, Harbin;
Tel.:+86 451 86412041; Email: P.Jin@hit.edu.cn

Abstract: In this paper, a double-layer aperiodic metallic grating is designed and the focusing performance is numerically researched using the finite-difference time-domain method. A sub-wavelength focusing spot is achieved and the depth of focus is twice the length of the incident wavelength. With its ease of fabrication, the designed aperiodic double-layer metallic grating has great potential in applications such as data storage, laser direct writing and optical probe.

Keywords: focusing performance, aperiodic grating, metallic subwavelength structure

1. Introduction

Breaking the optical diffraction limit to obtain sub-wavelength scale focusing spot has attracted considerable interest for applications in nano-lithography, laser direct writing, data storage, etc. [1,2,3,4,5,6,7,8,9,10,11,12]. Based on super oscillation theory, an optical planar mask with a quasi-crystal array of nanoholes was previously designed to achieve a super-resolution focusing spot [13]. However, its application was limited by the low energy efficiency. An alternative approach is the realization of sub-wavelength focusing based on surface plasmon polaritons (SPPs). In 2007, super-resolution was achieved in the visible frequency region using a super lens formed from a plasmonic microzone plate structure fabricated in a silver film [14]. In addition, radiation-less electromagnetic interference was proposed and shown experimentally to be capable of subwavelength focusing to $\lambda/20$ in the 1GHz range [15,16]. In 2010, a similar theory was used to design a near field focusing plate in the visible frequency region [17]. Unfortunately, the application of many nanoscale devices is limited by the inherent difficulty of their fabrication. For example, the maximum aspect ratio of the aforementioned focusing plate with sub-wavelength slit is as large as 50:1, which limits its realization [18].

In this paper, a double-layer aperiodic metallic grating is proposed to achieve super-resolution focusing while maintaining a much smaller aspect ratio. To study the designed grating structure, we employ the finite-difference time-domain method (FDTD Solutions, Lumerical Inc.) [19]. For incident light of wavelength 650 nm, a sub-wavelength focusing spot is obtained and the depth of focus (DOF) is twice the incident wavelength (1.37 μm). Most importantly, the difficulty of fabricating and assembling the device is greatly reduced due to the much smaller aspect ratio. The double-layer aperiodic metallic grating structure for sub-wavelength focusing therefore has a promising future for data storage, laser direct writing and optical probing.

2. Methods

To achieve a focal spot, the phase of the transmitted beam satisfies the equation:

$$\phi(y) = -\Delta\phi = 2n\pi + \frac{2\pi f}{\lambda} - \frac{2\pi\sqrt{f^2 + y^2}}{\lambda}\,. \tag{1}$$

where f and y represent the focal distance and the position of a slit along the y axis in Fig. 1(a), respectively. λ is the wavelength of the incident light in vacuum. The phase of the beam passing through the gold film can be controlled by the width of the slits, considering the generation of SPPs by the TM wave [18]. After passing through the grating structure, the beam will radiate into the space. The relation between the phase retardation in the slit and the slit parameters is determined by the following equation:

$$\tanh\left(\frac{w\sqrt{\beta^2 - k_0^2}}{2}\right) = \frac{-\sqrt{\beta^2 - k_0^2\varepsilon_m}}{\varepsilon_m\sqrt{\beta^2 - k_0^2}} \tag{2}$$

where w is the slit width of the metal film and β is the propagation constant of SPPs in the slit. k_0 is the propagation constant of the incident beam in vacuum, and ε_m is the relative permittivity of the metal. The real part of the complex quantity β determines the phase shift in the slit, while the imaginary part determines the energy loss. As is shown in Fig. 1(a), d is the thickness of the film. Thus βd is the phase shift of a beam travelling through the slit.

To obtain a high electric intensity at the focusing point, the thickness of the metallic film should be optimized. According to the previous research, the relation between the transmittance and thickness of the metallic film will satisfy the formula below [20]

$$E = \frac{E_i}{\pi}\frac{w}{t}\cos(\mathrm{k}_{SPP}\mathrm{t} + \frac{\pi}{2})\,. \tag{3}$$

where E_i is the electric intensity of the incident beam and t represents the thickness of the metal film. k_{SPP} is the propagation constant of SPPs. Fig. 1(b) is the transmission curve which shows a damped oscillatory tendency as the thickness of the metal film is increased from 100 nm to 800 nm.

As is shown in Fig. 1(b), despite the clear difference in transmission of gratings with different slit widths, the tendencies are consistent. For example, when a gold film with a thickness of 440 nm is illuminated by an incident beam with a wavelength of 650 nm, the transmission will reach a local maximum.

In addition, when a film with of thickness of d is composed of two films of thicknesses d_1 and d_2, so that d=d_1+d_2, a new relation for phase retardation is obtained as following:

$$\mathrm{Re}(\beta\,\mathrm{d}) = \mathrm{Re}(\beta\,\mathrm{d}_1) + \mathrm{Re}(\beta\,\mathrm{d}_2)\,. \tag{4}$$

Eq. 4 implies that the phase retardation is linear with the total thickness of the multi-layer structure. As an illustration, a film with a thickness of 440 nm is divided into two films with equal thickness. The transmission of this double-layer grating is calculated according to the intensity distribution curve. According to numerical calculations, the light coupling effect between the two layers can be neglected in designing the grating structure.

3. Results

To verify the assumption of the linear relation between the thickness of the multi-layer structure and the phase shift, a double-layer aperiodic gold grating structure was built and calculated by FDTD. The diagram of the double-layer aperiodic gold grating is shown in Fig. 2. The double-layer structure's lateral distribution of slits is exactly the same as that of a single-layer aperiodic grating with a thickness of d. The separation between the two layers along the x axis is 100 nm, represented by a. The dielectric layer is air and the separation between the slits is 60 nm, represented by s; the minimum width of the slit is 20 nm and the wavelength of the TM mode incident beam is 650 nm. According to the Drude-Lorentz model, the relative permittivity of gold is -12.9+1.2i [21] and the refractive index of air is 1.

The near field electric field intensity distribution of the double-layer grating is illustrated in Fig. 3. A focal point is shown at the transmitted side because of the phase modulation of the slits. In Fig. 4(a), the maximum electric field intensity occurs at x=2.9 μm. The maximum electric field intensity is 3.75 times that of the incident beam. The DOF, which is defined as the range having 80% of the maximum intensity, is 1.37 μm. The full width at half maximum (FWHM) is 533 nm, as shown in Fig. 4(b). Here the origin is chosen as the middle point of the second layer's exit facet. The FWHM at the focal plane is the same as that of a single layer, and the transmission remains the same. Therefore, the double-layer structure maintains the high focusing performance while significantly reducing the maximum depth-to-width ratio. In this case, the maximum required depth-to-width ratio is only 10:1.

4. Discussion

The tolerance of alignment of the two layers is calculated considering the lateral shift along x axis δx, the lateral shift along y axis δy and the rotation error $\delta\theta$. As shown in Fig. 5, the lateral shift along x axis, δx can be allowed to vary from -25 nm to 25 nm, while δy can be allowed to drift by as much as 20 nm. As for the rotation error, it can be seen from the simulation results that the requirement for the relative position between the two gold layers is relatively flexible. According to the alignment error tolerance calculation results shown in Table 1, the spot position and size both change slightly. The spot FWHM will see a slight increase as the front gold film moves along the x axis or rotates around its center. However, the coordinate of the focusing spot varies as the shift direction of the front film changes. The two dimensional electric field distributions for each case of alignment error are shown in Fig. 6. The distribution of electric field in different cases is nearly the same. According to the data analysis, the alignment error has a negligible impact on the focusing performance. As the double-layer structure is not sensitive to alignment error, we have more freedom to determine the method used for attaching the back layer to the front one. Here, we assume it is air filling in the slit and separation. Other materials such as adhesive can be used as the dielectric layer as well.

A wider slit width and gold wall should also increase the lateral shift error tolerance, for such structure reduces the fraction of light, which should have travelled through the wrong slits beside the target slit and then generated unexpected phases. A wider gold wall will increase the aperture of the metallic lens and the cost. A wider slit will result in a smaller phase retard, leading to the need for a thicker metallic film. Therefore, the minimum width of the structure and the lateral shift error tolerance should be balanced.

5. Conclusion

A double-layer aperiodic metallic grating has been designed and investigated theoretically. According to the simulation result, based on the FDTD method, both long DOF and spots with sub-wavelength FWHM are achieved simultaneously. As the required maximum depth-to-width ratio is half of that of a single layer with the same slit distribution, the proposed grating structure is easy to fabricate. Different types of alignment errors including the lateral shift along the *x* axis, the lateral shift along the *y* axis and the rotation error between layers and their influence on the focusing performance are discussed in detail. The proposed double-layer gold grating structure has the advantage of high focusing performance and ease of fabrication and assembly. It is expected to be widely used in data storage, laser direct writing and optical probe in the future.

Acknowledgements

This work is funded by National Natural Science Foundation of China (Grant no. 61008031, 61008039 and 51275111), the Program for New Century Excellent Talents in University (Grant NECT100059).

Table 1. The influence of alignment errors on the focusing performance

	Variation of x coordinate(nm)	Variation of y coordinate(nm)	FWHM(nm)
Designed structure	0	0	533
$\delta y = \pm 20$nm	0	± 8	533
$\delta x = \pm 25$nm	± 2	0	536 ± 3
$\delta\theta = \pm 1°$	± 2	± 8	534 ± 1

Figure Captions:

Fig. 1. (a) Schematic diagram of a single layer aperiodic gold grating. (b) Relation between normalized transmission and the thickness of the gold layer.

Fig. 2. Schematic diagram of the double-layer aperiodic gold grating. d_1 and d_2 represent the thickness of the two layers, respectively. a represents the separation of the two layers along x axis, and s represents the separation of slits.

Fig. 3. The near field electric field intensity distribution at the transmitted side of grating.

Fig. 4. (a) Electric field intensity along the x axis. (b) Electric field intensity along the y axis at the focal plane.

Fig. 5. Error factors of fabrication in aperiodic double-layers metallic grating. Lateral shift of the front layers along y axis is represented by δy . Vertical shift of the front layers along x axis is represented by δx . The rotation error between layers is represented by $\delta\theta$.

Fig. 6. Influence of the alignment error on the focusing effect: (a) electric field distribution in the case of a 20 nm lateral shift of the front layer, (b) electric field distribution in the case of δx =25 nm, (c) electric field distribution in the case of δx =-25 nm, (d) electric field distribution in the case of a 1 degree rotation of the front layer.

[1] T. W. Ebbesen, H. J. Lezec, H. F. Ghaemi, T. Thio, and P. A. Wolff, Extraordinary optical transmission through sub-wavelength hole arrays. Nature 1998, 391: 667-669.
[2] R. B. Greegor, C. G. Parazzoli, and M. H. Tanielian, Origin of dissipative losses in negative index of refraction materials. Applied Physics Letters 2003, 82(14): 2356–2358.
[3] D. Melville, and R. Blaikie, Super-resolution imaging through a planar silver layer. Optics Express 2005, 13(6): 2127–2134.
[4] X. Zhang, and Z. Liu, Superlenses to overcome the diffraction limit. Nature materials 2008, 7: 435-441.
[5] W. C. Cheong, B. P. S. Ahluwalia, X. C. Yuan, L. S. Zhang, H. Wang, H. B. Niu, and X. Peng, Fabrication of efficient microaxicon by direct electron-beam lithography for long nondiffracting distance of Bessel beams for optical manipulation. Applied Physics Letters 2005, 87(2): 024104-024104-3.
[6] D. Z. Lin, C. H. Chen, C. K. Chang, T. D. Cheng, Subwavelength nondiffraction beam generated by a plasmonic lens. Applied Physics Letters 2008, 92(23): 233106-233106-3.
[7] D. K. Gramotnev, and S. I. Bozhevolnyi, Plasmonics beyond the diffraction limit. Nature photonics 2010, 4: 83-91.
[8] G. Bartal, G. Lerosey, and X. Zhang, Subwavelength dynamic focusing in plasmonic nanostructures using time reversal. Physical Review B 2009, 79(20): 201103-1-201103-4.
[9] A. Grbic, and G. V. Eleftheriades, Overcoming the diffraction limit with a planar left-handed transmission-line lens. Physical Review Letters 2004, 92(11): 117403-117406.
[10] Z. Liu, S. Durant, H. Lee, Y. Pikus, N. Fang, Y. Xiong, C. Sun, and X. Zhang, Far-field optical superlens. Nano Letters 2007, 7(2): 403–408.
[11] J. Lin, K. Yin, Y. Li, and J. B. Tan, Achievement of longitudinally polarized focusing with long focal depth by amplitude modulation. Optics Letters 2011, 36(7): 1185-1187.
[12] N. Gao, and C. Xie, High-order diffraction suppression using modulated groove position gratings. Optics Letters 2011, 36(21): 4251-4253.
[13] F. M. Huang, and N. I. Zheludev, Super-Resolution without Evanescent Waves. Nano Letters 2009, 9(3): 1249-1254.
[14] Y. Fu, W. Zhou, L. E. N. Lim, and C. L. Du, Plasmonic microzone plate: Superfocusing at visible regime. Applied Physics Letters, 2007, 91(6): 061124(1)-061124(3).
[15] R. Merlin, Radiationless electromagnetic interference: Evanescent-field lenses and perfect focusing. Science 2007, 317(5840): 927-929.
[16] A. Grbic, L. Jiang, and R. Merlin, Near-field plates: Subdiffraction focusing with patterned surfaces. Science 2008, 320(5875): 511-513.
[17] H. F. Shi, and L. J. Guo, Design of plasmonic near field plate at optical frequency. Applied Physics Letters 2010, 96(14): 141107-1-141107-3.
[18] H. Shi, C. Wang, C. Du, X. Luo, X. Dong, and H. Gao. Beam manipulating by metallic nano-slits with variant widths. Optics Express 2005, 13(18): 6815–6820.
[19] http://www.lumerical.com/tcad-products/fdtd/
[20] F. A. Ferri, V. A. G. Rivera, S. P. A. Osorio, O. B. Silva, A. R. Zanatta, B. H. V. Borges, John Weiner, and Euclydes Marega, Jr. Influence of film thickness on the optical transmission through subwavelength single slits in metallic thin films. Applied Optics 2011, 50(31): G11-G16.
[21] A. Vial, A. S. Grimault, D. Macías, D. Barchiesi, and M. L. Chapelle, Improved analytical fit of gold dispersion: application to the modeling of extinction spectra with a finite-difference time-domain method. Physics Review B 2005, 71(8): 085416-085422.

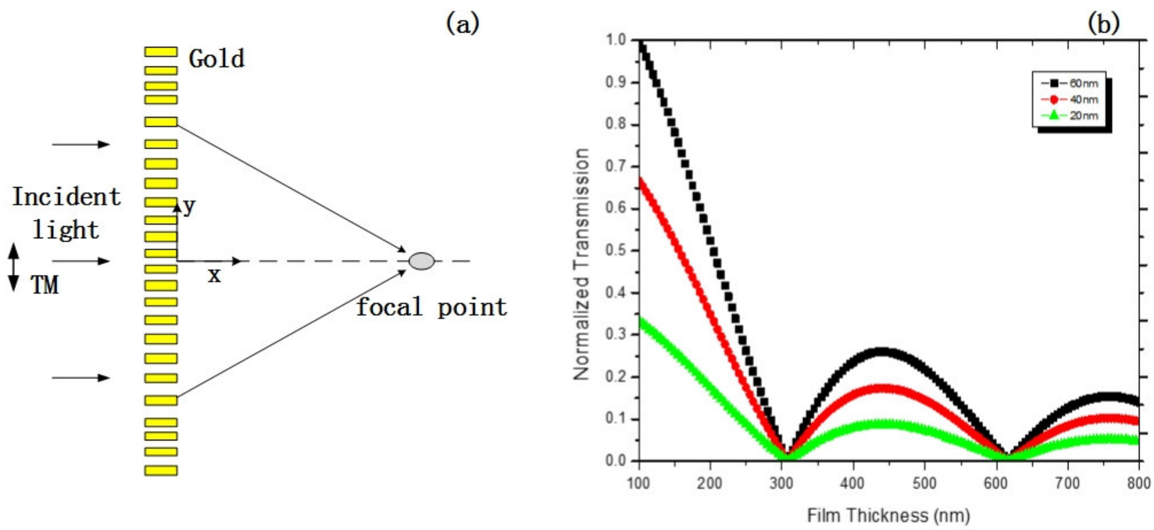

(a)
Gold
Incident light
TM
y
x
focal point
(b)
60nm
40nm
20nm
Normalized Transmission
Film Thickness (nm)

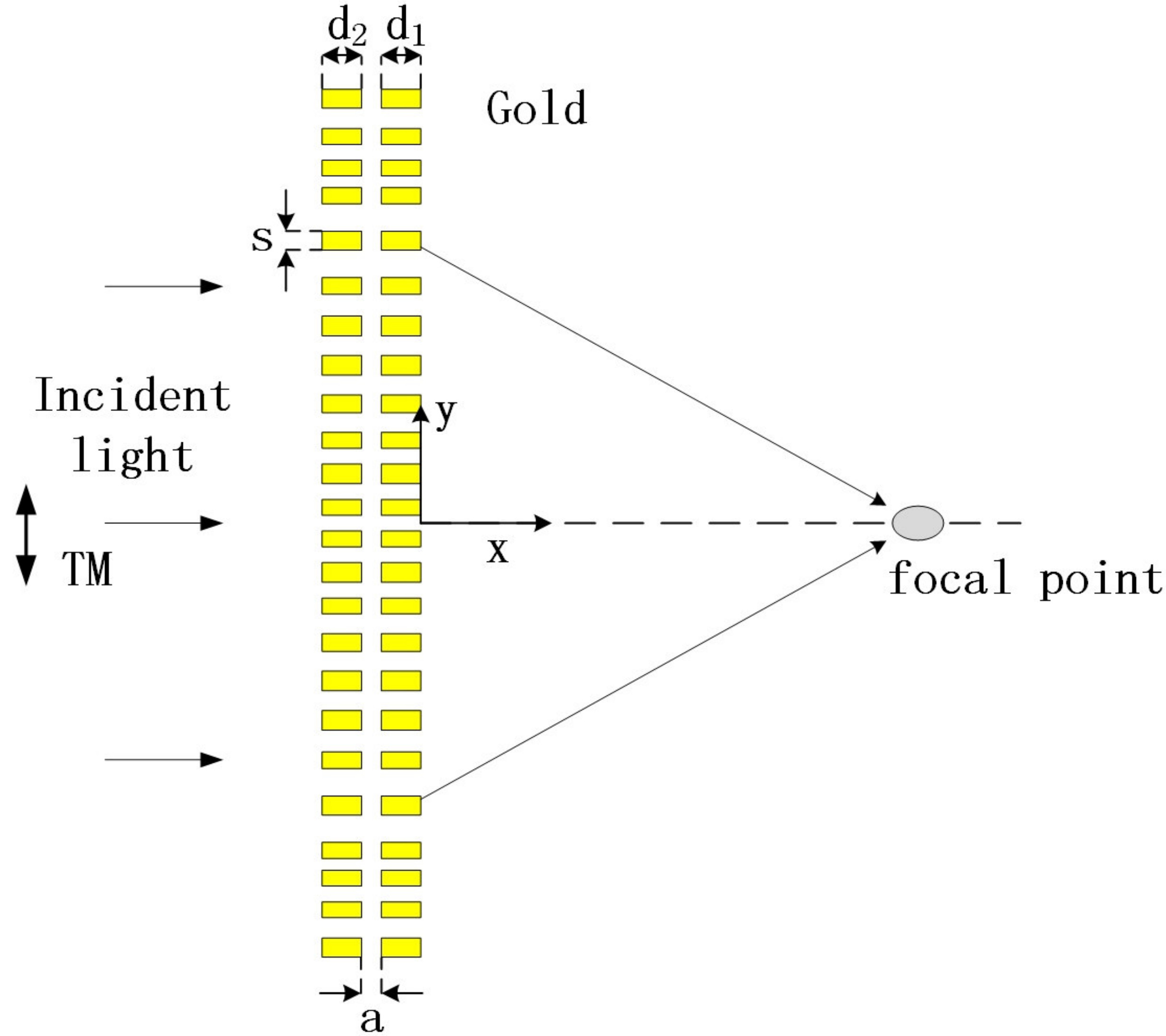

d2
d1
Gold
s
Incident
light
TM
y
x
focal point
a

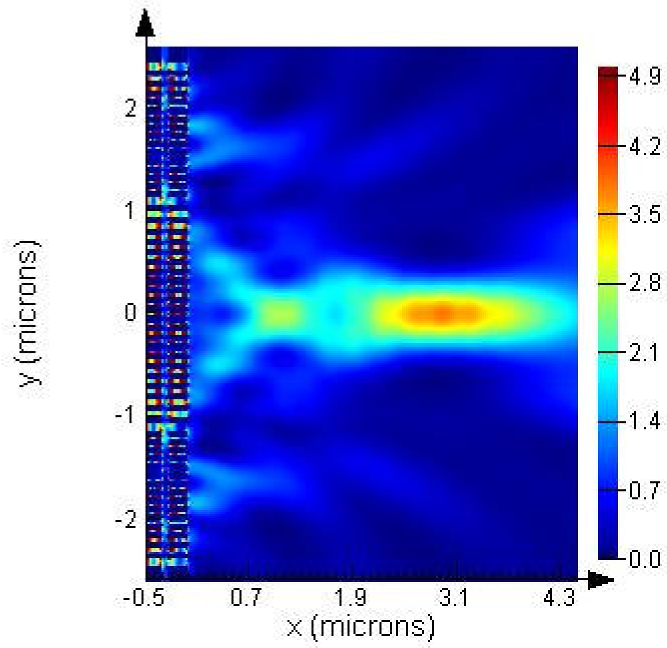

y (microns)
2
1
0
-1
-2
-0.5
0.7
1.9
3.1
4.3
x (microns)
4.9
4.2
3.5
2.8
2.1
1.4
0.7
0.0

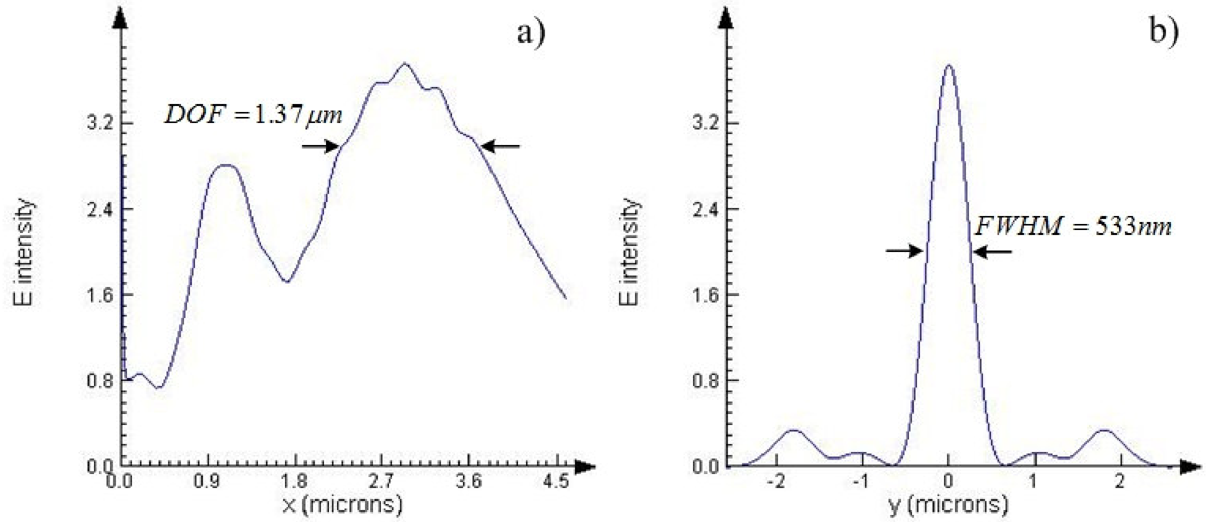
a)
DOF = 1.37 μm
E intensity
3.2
2.4
1.6
0.8
0.0
0.0
0.9
1.8
2.7
3.6
4.5
x (microns)
b)
FWHM = 533nm
E intensity
3.2
2.4
1.6
0.8
0.0
-2
-1
0
1
2
y (microns)

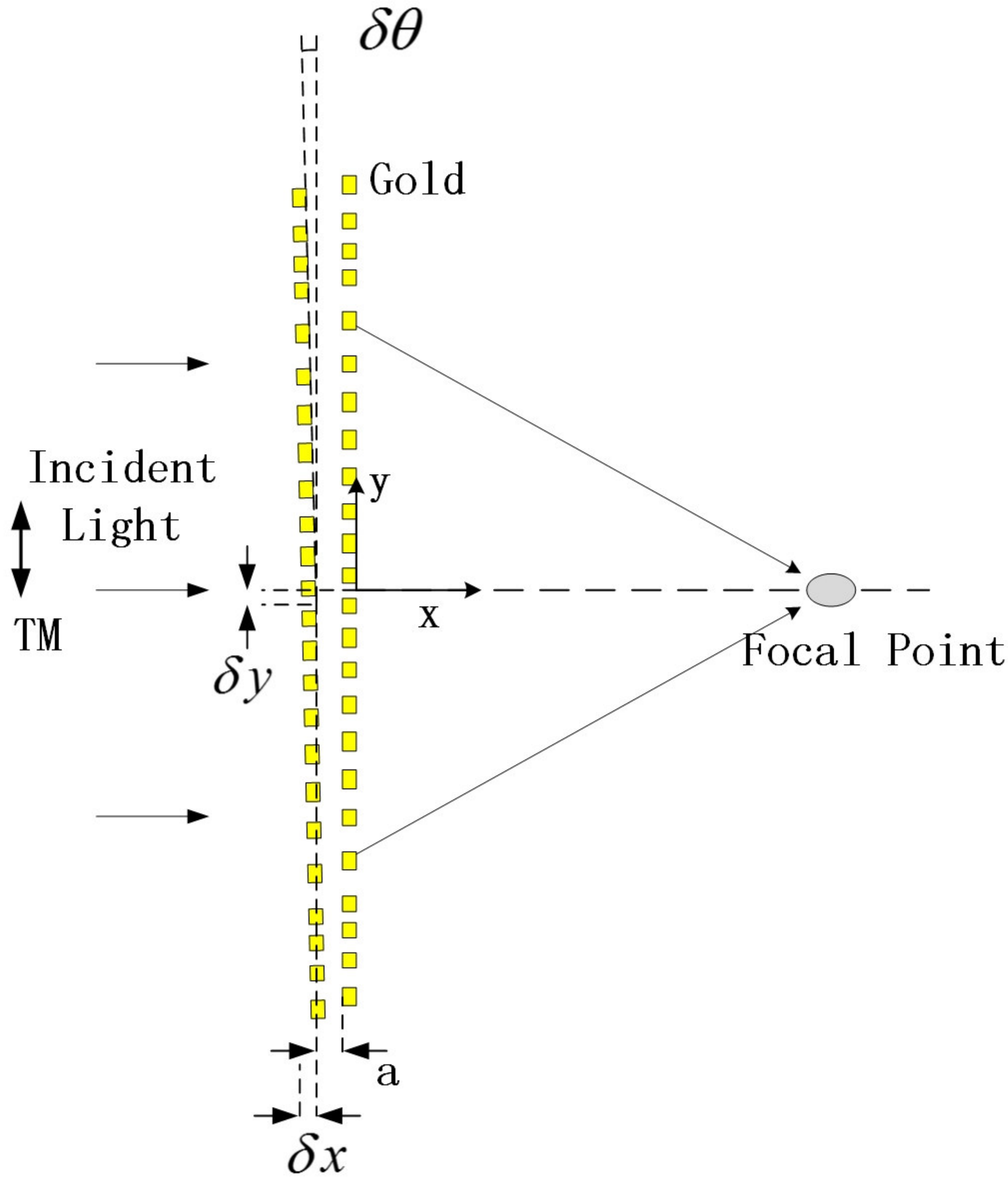

$\delta\theta$
Gold
Incident
Light
TM
y
x
δy
Focal Point
a
δx

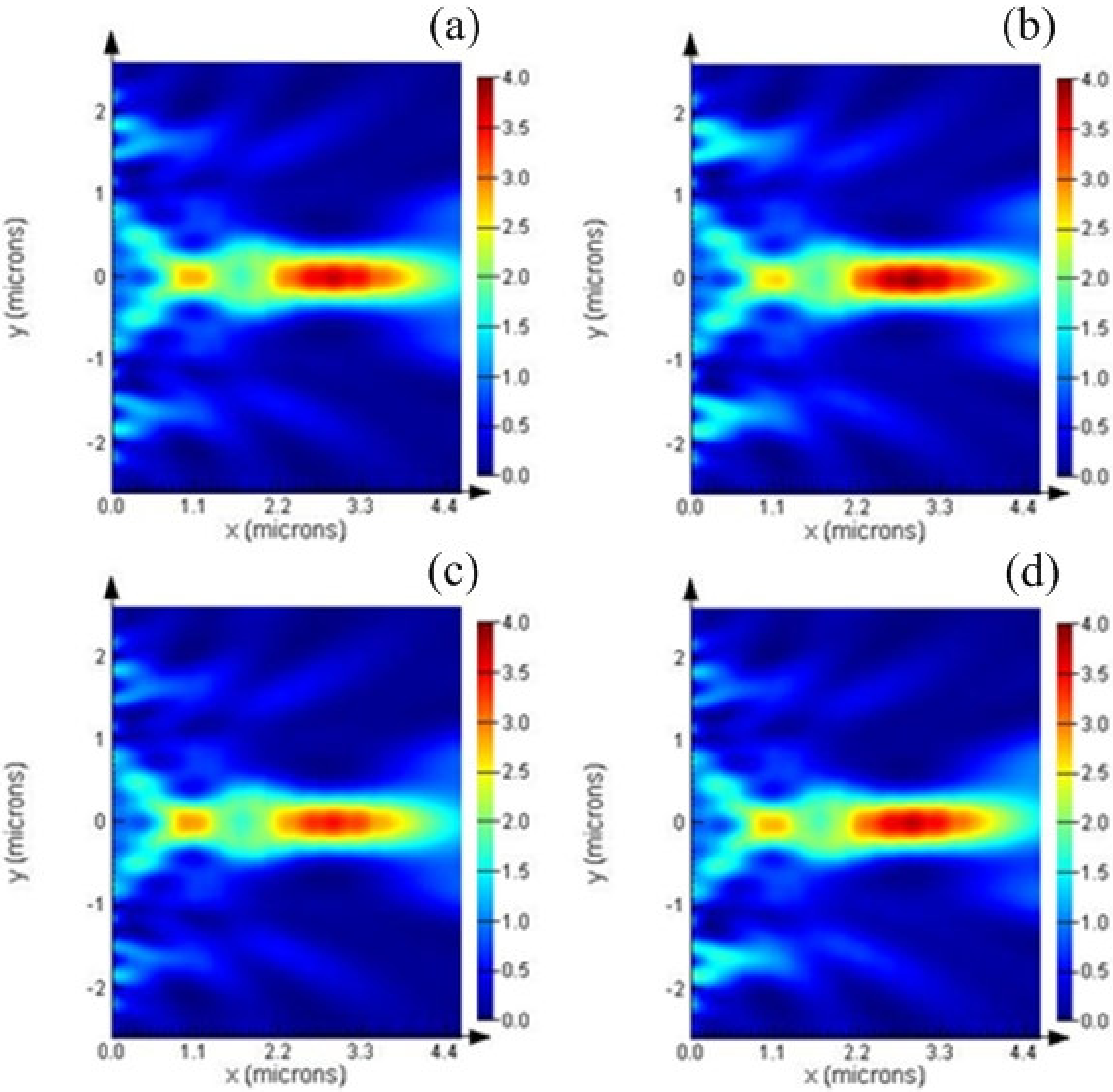

(a)
(b)
(c)
(d)
y (microns)
x (microns)
0.0
1.1
2.2
3.3
4.4
2
1
0
-1
-2
4.0
3.5
3.0
2.5
2.0
1.5
1.0
0.5
0.0

y (microns)
2
1
0
-1
-2
-0.5
0.7
1.9
3.1
4.3
x (microns)
4.9
4.2
3.5
2.8
2.1
1.4
0.7
0.0
δθ
Gold
Incident
Light
TM
δy
y
x
Focal Point
a
δx

An aperiodic double layer metallic grating is designed.

A subwavelength and long depth of focus focal spot is achieved.

Focusing performance is insensitive to alignment errors between layers.